

## Metal Ion Assisted Folding and Supramolecular Organization of a De Novo Designed Metalloprotein

Guido W. M. Vandermeulen,<sup>A</sup> Christos Tziatzios,<sup>B</sup> Dieter Schubert,<sup>B</sup> Philip R. Andres,<sup>C</sup> Alexander Alexeev,<sup>C</sup> Ulrich S. Schubert,<sup>C</sup> and Harm-Anton Klok<sup>D,E</sup>

<sup>A</sup> Max Planck Institute for Polymer Research, 55128 Mainz, Germany.

<sup>B</sup> Johann Wolfgang Goethe-Universität, Institut für Biophysik, 60590 Frankfurt am Main, Germany.

<sup>C</sup> Eindhoven University of Technology and Dutch Polymer Institute, Laboratory of Macromolecular Chemistry and Nanoscience, 5600 MB Eindhoven, The Netherlands.

<sup>D</sup> École Polytechnique Fédérale de Lausanne, Laboratoire des Polymères, Institut des Matériaux, 1015 Lausanne, Switzerland.

<sup>E</sup> Author to whom correspondence should be addressed (e-mail: Harm-Anton.Klok@epfl.ch).

This paper describes the supramolecular organization of a novel de novo designed metalloprotein, which consists of two *N*-terminal terpyridine modified coiled-coil protein folding motif sequences held together by an iron(II) ion. The self-assembly of the metalloprotein is the result of the interplay of metal ion complexation and protein folding, and can be manipulated by changes in concentration, temperature, and solvent. At low concentrations, folding and organization of the metalloprotein resembles that of the native coiled-coil peptide. Besides unimeric species, also dimeric and tetrameric metalloprotein assemblies were found. Several indications suggest that at least part of these unimeric species may exist as intramolecularly folded coiled-coils, however, unambiguous proof is lacking at the moment. At higher concentrations, folding and organization is dominated by the large octahedral [Fe<sup>II</sup>(terpy)<sub>2</sub>] complexes (terpy = 2,2':6',2''-terpyridine) and considerable amounts of large, ill-defined aggregates are formed.

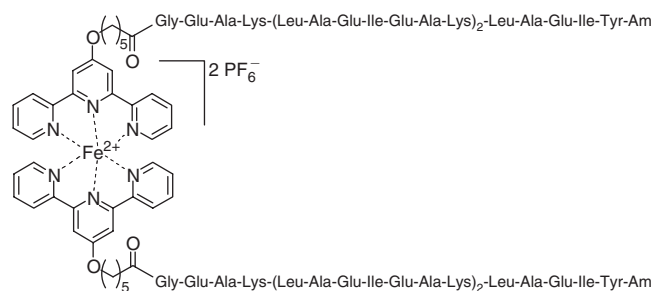
Manuscript received: 26 September 2003.

Final version: 30 October 2003.

### Introduction

Metal ions play an important role in defining the three-dimensional structure of native metalloproteins,<sup>[1]</sup> such as in DNA-binding zinc finger proteins,<sup>[2]</sup> and are used by nature to perform a wide variety of specific functions, for example electron transfer and the binding and activation of substrates for enzymes. De novo designed minimalistic metalloproteins are useful tools for gaining insight into the structure–property relationships of metalloproteins. Artificial metalloproteins can be obtained by introducing metal coordinating groups either to the *N*- or *C*-terminus of a peptide chain or in the side chains of the constituent  $\alpha$ -amino acids. In most of the work published so far, metal ion complexation was exclusively used to direct the formation of well-defined tertiary structures. Examples of tertiary structures, which have been generated using metal complexation as the driving force, include two- and three-stranded  $\alpha$ -helical coiled-coils,<sup>[3,4]</sup> two-, three-, and four-helix bundles,<sup>[5–7]</sup> and collagen triple helices.<sup>[8]</sup>

In most of the studies published so far, the influence of metal complexation and its interplay with protein folding on the possible formation of larger quaternary assemblies has been largely neglected. In most cases, the experiments focussed on the low concentration regime where the formation of supramolecular structures from metalloproteins



Scheme 1. Structure of the metalloprotein.

does not play a role. In this paper, we present the results of a concentration dependent study of the folding and organization of a de novo metalloprotein. Instead of solely using metal complexation to direct the formation of well defined protein tertiary structures, we sought to explore the interplay between protein folding and metal complexation in order to manipulate both tertiary structure and supramolecular organization. The artificial protein discussed in this contribution consists of two identical coiled-coil peptide sequences and an octahedral terpyridine metal complex (Scheme 1). The coiled-coil motif consists of two to five peptide helices that are wrapped around each other into a superhelix.<sup>[9]</sup> The terpyridine moiety has outstanding complexation properties for a wide range of

transition metal ions and has been extensively used in recent years to construct a wide range of defined macromolecular assemblies based on synthetic building units.<sup>[10]</sup>

## Results and Discussion

The primary structure of the metalloprotein is a de novo designed  $\alpha$ -amino acid sequence, which is known to induce folding into dimeric and tetrameric coiled-coil superstructures.<sup>[11]</sup> The terpyridine modified coiled-coil apo-peptides were prepared by standard Fmoc solid-phase peptide synthesis, using 6-(2,2':6',2''-terpyridin-4'-yloxy)hexanoic acid<sup>[12]</sup> as the *N*-terminal capping agent. Functionalization of the terpyridine at the central 4'-position affords a symmetric ligand, which avoids additional complexity in analyzing the folding behaviour due to the possible formation of different diastereoisomers. After dialysis, MALDI-TOF (matrix-assisted laser desorption-ionization time-of-flight) mass spectrometry identified the purified compound as the desired apo-peptide and, according to reverse phase HPLC analysis, the apo-peptide had a purity of  $\geq 95\%$  (see Accessory Materials). Addition of  $\text{FeSO}_4 \cdot 7\text{H}_2\text{O}$  to a methanolic solution of the apo-peptide followed by an excess of  $\text{NH}_4\text{PF}_6$  yielded the corresponding  $\text{Fe}^{\text{II}}$  hexafluorophosphate complex.

Complex formation between the apo-peptide and  $\text{Fe}^{\text{II}}$  was evidenced by UV-vis spectroscopy. As shown in Fig. 1, complex formation results in a red shift of the terpyridine  $\pi$ - $\pi^*$  band to 329 nm and the appearance of a new absorption band with  $\lambda_{\text{max}}$  at 561 nm, which represents the metal-to-ligand charge transfer (MLCT) transition.<sup>[13]</sup> According to UV-vis spectroscopy, metal complexation yields assemblies which are rather insensitive to changes in concentration, solvent (aqueous, acidic, and organic), and pH. Evidence for decomplexation was only found in aqueous solution above pH 11 (spectra in Accessory Materials) and at very high pressures during RP-HPLC analysis, which is a known phenomenon for terpyridine transition metal complexes.<sup>[14]</sup> The dimeric character of the metalloprotein was supported by MALDI-TOF mass spectrometry (Fig. 2a). The major signal at 5750 Da in the MALDI-TOF mass spectrum corresponds to the sum of the masses of two terpyridine-containing apo-peptides and one  $\text{Fe}^{\text{II}}$  ion. The presence of the MALDI-TOF signals with higher molecular weights than that of the  $\text{Fe}^{\text{II}}$  complex is due to the exchange of acidic protons of L-glutamic acid residues with sodium, which was added as a salt to facilitate ionization. Further evidence for the quantitative  $\text{Fe}^{\text{II}}$  complexation was obtained from GPC (gel permeation chromatography) analysis (Fig. 2b). The reduced GPC elution time of the  $\text{Fe}^{\text{II}}$  complex in comparison with the terpyridine-modified apo-peptide reflects the higher molecular weight of the  $\text{Fe}^{\text{II}}$  complex.

The folding behaviour and supramolecular organization of the metalloprotein was investigated by circular dichroism (CD) spectroscopy and analytical ultracentrifugation (AUC) and compared with that of the apo-peptide and the native coiled-coil sequence. The concentration dependence of the helix content and the ratio of molar ellipticities at 222 and 208 nm, which can be calculated from the CD spectra (see Accessory Material),<sup>[15]</sup> are shown in Fig. 3.

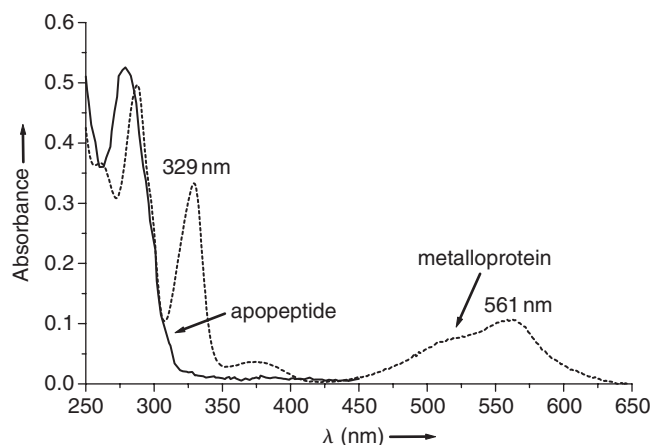


Fig. 1. UV-vis spectra of the apo-peptide (—) and metalloprotein (---) in PBS, pH 7.4.

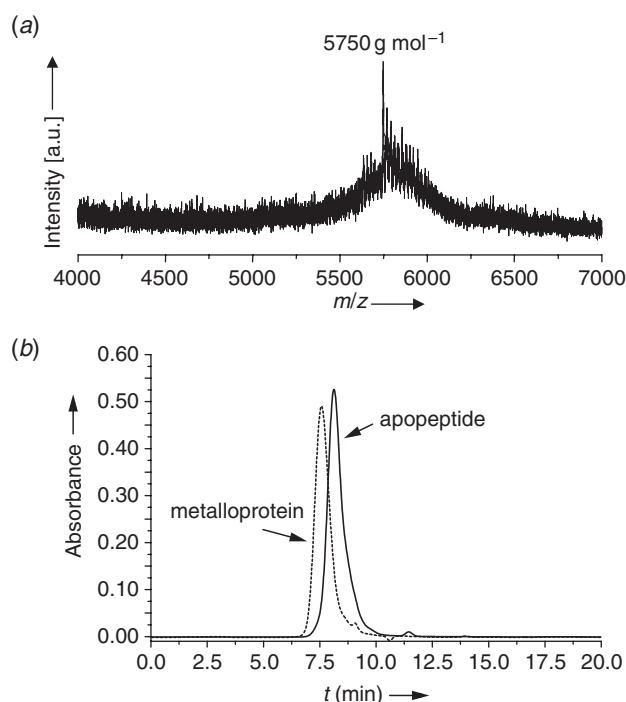
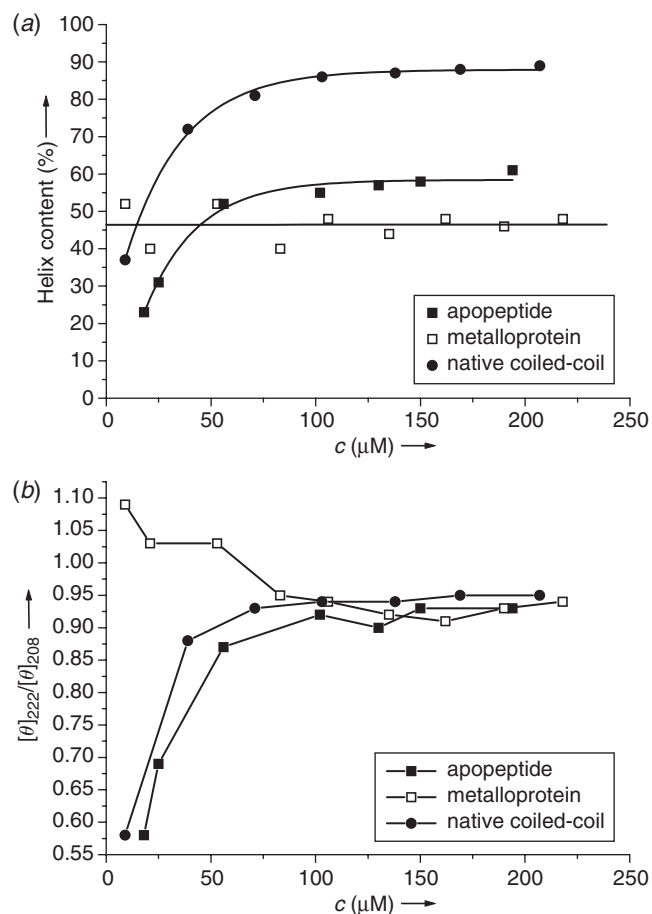


Fig. 2. (a) MALDI-TOF mass spectrum of the metalloprotein; (b) GPC traces of the apo-peptide (—) and the metalloprotein (---).

The folding behaviour of the native coiled-coil has been reported in detail before and can be described in terms of an equilibrium between partially folded unimers and dimeric and tetrameric coiled-coil assemblies.<sup>[11]</sup> The plateau value of approximately 0.95 for  $[\theta]_{222}/[\theta]_{208}$  is characteristic for coiled-coil superstructures, and the concentration dependence of the helix content reflects the increasing relative amounts of coiled-coil assemblies formed at higher concentrations.<sup>[16]</sup> Qualitatively, the results of CD experiments on the terpyridine-containing apo-peptide and the native coiled-coil sequence are identical. The lower helix content of the apo-peptide could reflect the steric hindrance of the terpyridine moieties, which would reduce the relative amount of folded assemblies in solution, but could also be an underestimate of the true value due to the interference of



**Fig. 3.** Plots showing the concentration dependence of (a) the helix content; and (b) the ellipticity ratio  $[\theta]_{222}/[\theta]_{208}$  for the native coiled-coil, the apopeptide, and the metalloprotein.

CD-active bands from the attached terpyridine.<sup>[17]</sup> According to AUC experiments, the self-organization of the terpyridine-containing apopeptide can also be described in terms of an equilibrium between partially folded unimers and dimeric and tetrameric coiled-coil assemblies. Apart from a few percent of octamers, no larger aggregates were observed.

The results of the concentration-dependent CD experiments on the metalloprotein point towards a folding behaviour that is distinctly different from that of the native coiled-coil and the apopeptide. First of all, the helix content is relatively low (approximately 45%) and concentration independent. The relatively low helix content may be due to the steric hindrance of the large  $\text{Fe}(\text{tpy})_2$  complex attached to a relatively short peptide, but could also be influenced due to interference of the CD-active bands from the attached  $[\text{Fe}(\text{terpy})_2]$ .<sup>[17]</sup> Furthermore, a remarkable concentration dependence of the ratio of molar ellipticities at 222 and 208 nm is observed. At low concentrations ( $<50 \mu\text{M}$ ), a  $[\theta]_{222}/[\theta]_{208}$  ratio of approximately 1.0–1.1 can be observed. At higher concentrations,  $[\theta]_{222}/[\theta]_{208}$  decreases and reaches a plateau value of approximately 0.95 between 100 and 200  $\mu\text{M}$ , similar to the apopeptide and the native coiled-coil sequence.

Analytical ultracentrifugation experiments carried out at sample concentrations of 31, 78, and 118  $\mu\text{M}$  indicated the

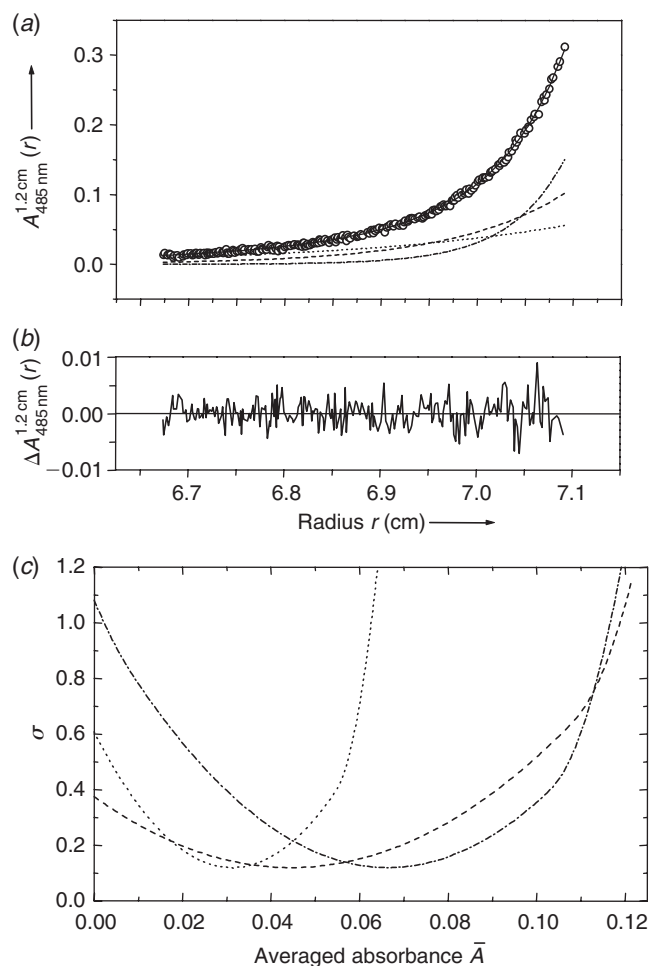


**Fig. 4.** Sedimentation equilibrium analysis of the  $\text{Fe}^{\text{II}}$  complex at a concentration of 78  $\mu\text{M}$ . (a) Experimental absorbance versus radius data  $A_{485 \text{ nm}}^{1.2 \text{ cm}}(r)$ ; best fit to the data based on  $\bar{v} = 0.776 \text{ mL g}^{-1}$  and a unimer molar mass of  $6040 \text{ g mol}^{-1}$  assuming a unimer–dimer–tetramer model of self-association (—), and calculated local contributions of unimers ( $\cdots$ ), dimers (---), and tetramers (— · — · —). (b) Local differences  $\Delta A_{485 \text{ nm}}^{1.2 \text{ cm}}(r)$  between experimental and calculated  $A(r)$  data. (c) Statistical accuracy of the calculated absorbance contributions of the different oligomers: changes in the sum of the squared residuals ( $\sigma$ ) of fits to the data from Fig. 5a, which result from one non-optimal absorbance parameter.<sup>[19]</sup> The minima of the curves represent the best-fit figures for the content of the sample of each oligomer.

presence of unimeric metalloprotein, as well as dimeric and tetrameric aggregates (Fig. 4 and Table 1). We define an unimeric metalloprotein as one  $[\text{Fe}^{\text{II}}(\text{terpy})_2]$  core flanked by two peptide chains. Because the plateau value of  $[\theta]_{222}/[\theta]_{208}$  in the concentration regime between 100–200  $\mu\text{M}$  is identical to that of the native coiled-coil sequence and of the apopeptide, and since the formation of coiled-coil superstructures in the latter cases is the result of an intermolecular folding process, we propose that the dimeric and tetrameric metalloprotein assemblies detected by AUC are also formed by the assembly of intermolecular coiled-coils, as illustrated in Fig. 5. Since the native coiled-coil sequence also forms dimeric and tetrameric assemblies, which are in equilibrium with partially folded unimers, these results demonstrate that the self-assembly properties of the peptide sequences are largely retained after introduction of the terpyridine moiety

**Table 1. Results from sedimentation equilibration analysis of the metalloprotein**

U = unimer, D = dimer, T = tetramer, LA = large aggregate

Conc. [ $\mu\text{M}$ ]	Solvent	U content [%]	D content [%]	T content [%]	LA content [%]
31	100% PBS	$16 \pm 2$	$31 \pm 3$	$45 \pm 1$	8
78	100% PBS	$10 \pm 1$	$11 \pm 2$	$21 \pm 1$	58
118	100% PBS	$7 \pm 1$	$3 \pm 1$	$27 \pm 2$	63
33	50% PBS in ethanol	$66 \pm 1$	$0 \pm 1$	$1 \pm 1$	33

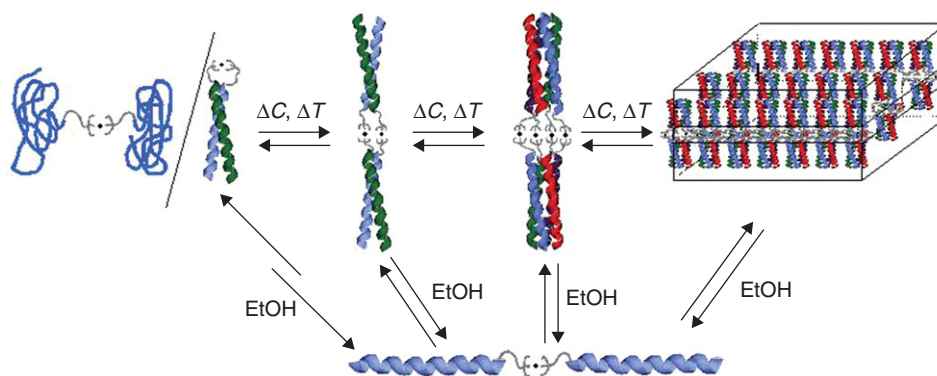


**Fig. 5.** Proposed model for the self-assembly of the metalloprotein. Unimers are depicted as being composed of either two unordered peptide sequences and/or an intramolecularly folded coiled-coil. At the moment, there is not sufficient experimental evidence to determine which of these structures is present, or whether they may coexist.

and metal complexation. In addition to unimeric metalloproteins and dimeric and tetrameric assemblies, the samples at 78 and 118  $\mu\text{M}$  were also found to contain a considerable fraction (approximately 60%) of large aggregates. Even at low rotor speed, these aggregates readily sedimented to the bottom of the centrifuge cell. Due to sample heterogeneity, CD spectroscopy can probably only detect the unimeric, dimeric, and tetrameric metalloproteins.<sup>[18]</sup> The large aggregates, which have an hydrodynamic radius of approximately 100 nm according to dynamic light scattering (DLS) experiments, may suffer from absorbance flattening effects and do therefore not contribute significantly to the CD spectra. A possible explanation for the unspecific association of the metalloprotein into large aggregates may be the relatively hydrophobic nature of the  $\text{Fe}^{\text{II}}$ -terpyridine complex with hexafluorophosphate counter ions. In addition, ionic interactions should be taken into consideration.

The concentration dependence of the oligomer contents (Table 1) suggests the presence of an association equilibrium between the oligomers. So far, however, efforts to unambiguously demonstrate its existence failed; the association behaviour of the samples seems to be very complex. Probably, part of the material forms, by unknown reasons, stable or metastable aggregates.

Further indications for the non-specific aggregation of the metalloprotein at high concentration were obtained from first non-contact mode atomic force microscopy (AFM) experiments. As an example, Fig. 6 shows the AFM phase images of thin layers of the apo-peptide and the metalloprotein, which were obtained by drop-casting from methanol solution. In the case of the apo-peptide, extended linear strands with a diameter of approximately 20 nm can be observed.

These strands are probably aggregates of a large number of coiled-coil superstructures. In contrast to the superstructures formed by the apo-peptide, the AFM image of the metalloprotein only features ill-defined flat domains with a diameter of 500–1000 nm. These AFM images reflect the results of the AUC experiments, which also indicated that the apo-peptide self-assemble into defined superstructures, while the metalloprotein also aggregates into large undefined assemblies.

In the case of the native coiled-coil sequence and the apo-peptide, decreasing the sample concentration to below 50  $\mu\text{M}$  shifts the equilibrium from folded superstructures to unfolded unimers, which is reflected in a decrease in both the helix content and  $[\theta]_{222}/[\theta]_{208}$ . For the metalloprotein, however, the helix content does not change with decreasing concentration. The reason for this is not clear at the moment; one tempting interpretation could be the formation of intramolecularly folded unimeric metalloproteins, which would be promoted by the intrinsic instability of the amphiphilic peptide sequences in their unimeric form and their high local concentration due to metal-ion complexation. The large terpyridine–metal complex could lead to fringing at the coiled-coil's *N*-terminus, which may explain the increase in  $[\theta]_{222}/[\theta]_{208}$  from 0.95 to 1.0–1.1 at concentrations below 50  $\mu\text{M}$ . The AUC data summarized in Table 1, however, also indicate that decreasing the concentration, especially below 50  $\mu\text{M}$ , results in a decrease in the fraction of large aggregates, which probably do not contribute to the CD signal. An alternative explanation of the concentration independence of the helix content would assume that the unimeric metalloproteins are composed of unordered peptide sequences and that the loss in the CD signal due to the



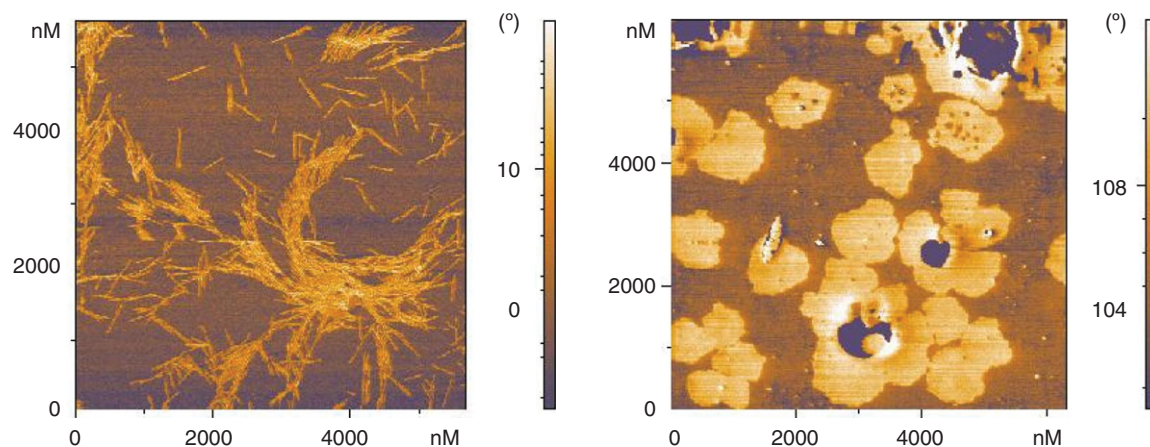


Fig. 6. AFM phase images of thin layers of the apo-peptide (left) and metalloprotein (right).

increasing amount of unfolded unimers at low concentration is compensated for by the increasing amounts of dimeric and tetrameric species, which, in contrast to the large aggregates, do contribute to the CD intensity. At this moment, it is not possible to determine which of these two explanations is more plausible, or whether both play a role.

In addition to concentration, the folding and organization of the metalloprotein can also be manipulated by addition of ethanol. As seen in Table 1, AUC experiments revealed that the addition of 50% ethanol resulted in dissociation of dimeric and tetrameric assemblies into unimeric metalloproteins. Further evidence for the disruption of the metalloprotein tertiary and quaternary structures in the presence of 50% ethanol is obtained from CD spectroscopy, which showed a decrease of  $[\theta]_{222}/[\theta]_{208}$  to approximately 0.85 (see Accessory Material). The  $\alpha$ -helical character of the two peptide sequences which constitute the metalloprotein is, however, retained upon disruption of the tertiary structure. The helix content of the metalloprotein in 50% ethanol was found to be only approximately 15% higher than in 100% phosphate-buffered saline solution. This small increase indicates that the peptides are already folded with a close-to-maximum helix content in 100% PBS, which is a further indication of the steric hindrance of the large octahedral  $[\text{Fe}(\text{terpy})_2]$  complex on the folding of the relatively short peptide sequence, but could also support the hypothesis that the observed helix contents are underestimated due to a possible interference effect of CD-active bands from the attached  $[\text{Fe}(\text{terpy})_2]$ .<sup>[17]</sup>

In contrast to the addition of ethanol, which simultaneously disrupts tertiary and quaternary structure, but stabilizes secondary structure, an increase in temperature results in both dissociation and unfolding, i.e. full denaturation, of the metalloprotein. This was evidenced by thermal denaturation CD experiments, which indicated both a decrease in  $[\theta]_{222}/[\theta]_{208}$  and a decrease in helix content with increasing temperature (see Accessory Material).

## Conclusions

The results described in this contribution demonstrate that the structure and organization of the de novo designed

metalloprotein is not exclusively dictated by metal ion complexation, but is the result of the interplay of metal ion complexation and protein folding. CD and AUC experiments indicated that the folding properties of the peptide sequences are retained after introduction of the terpyridine ligand and metal complexation. At low concentration, folding and organization of the metalloprotein was reminiscent to that of the native coiled-coil. In addition to unimeric species, dimeric and tetrameric metalloprotein assemblies were also found. Although this could not be unequivocally proven, there are several indications which suggest that, at least part of, the unimeric metalloproteins consist of an intramolecularly folded coiled-coil. At high concentrations, the association behaviour of the metal ion complexes dominates the folding properties and leads to large supramolecular metalloprotein assemblies.

## Experimental

### Materials

Amino acids, resins, *O*-benzotriazole-*N,N,N',N'*-tetramethyluronium hexafluorophosphate (HBTU), and *N*-hydroxybenzotriazole (HOBT) were purchased from Calbiochem–Novabiochem GmbH (Schwalbach, Germany). NMP was obtained from BASF AG (Ludwigshafen, Germany). All other chemicals and reagents were acquired from Sigma Aldrich Chemie GmbH (Deisenhofen, Germany). 6-(2,2':6',2''-Terpyridin-4'-yloxy)hexanoic acid was prepared according to a literature procedure.<sup>[12]</sup> NMP and DMF were dried over molecular sieves (4 Å) before use. Spectra/Por® dialysis bags (made from regenerated cellulose) were purchased from Carl–Roth GmbH (Karlsruhe, Germany).

### MALDI-TOF Mass Spectrometry

MALDI-TOF mass spectra were recorded on a Bruker Reflex II MALDI-TOF spectrometer. The apo-peptide was dissolved in tetrahydrofuran (THF) and mixed with the matrix 2,5-dihydroxybenzoic acid (DHB). Sodium trifluoroacetate was added to facilitate ionization. Sample preparation for bis(apo-peptide) iron(II) hexafluorophosphate was carried out according to a published procedure.<sup>[20]</sup>

### Reverse-Phase High-Pressure Liquid Chromatography (RP-HPLC)

RP-HPLC was performed on an Applied Biosystems Biocad Sprint workstation, using a Macherey Nagel C<sub>18</sub> reverse-phase column (EC 250/4 NUCLEOSIL, 500 Å pore size, 5 μM particle size). Samples were

eluted with a linear AB gradient from A to B over 20 min, with A consisting of 80 : 20 (v/v) water/acetonitrile (plus 0.1% TFA) and B of 100% acetonitrile (plus 0.1% TFA). The flow rate was 0.7 mL min<sup>-1</sup>. Sample elution was monitored with a UV-vis detector at 210 nm.

#### Gel Permeation Chromatography

GPC was performed on an Applied Biosystems Biocad Sprint workstation, using a Macherey Nagel 1102911 HEMA column (10 μm particle size, 100–1 000 000 Å pore sizes). Samples were eluted with a 1 : 1 (v/v) mixture of water and acetonitrile containing 0.2% TFA. The flow rate was 1.0 mL min<sup>-1</sup>. Sample elution was monitored with a UV-vis detector at 210 nm.

#### Sample Preparation for UV-Vis, DLS, CD, and AUC Experiments

The apo-peptide and metalloprotein were dissolved in PBS buffer (pH 7.4), stirred for approximately 1 h, and sonicated for a few minutes. The samples were centrifuged (15 000 rpm, 30 min) and the supernatants were used in the experiments. Sample preparation was performed at room temperature.

#### UV-Vis Spectroscopy

UV-vis spectra were recorded on a Perkin Elmer Lambda 15 spectrophotometer. Molar extinction coefficients were determined by measurement of samples with known concentration in PBS, pH 7.4. Concentrations were calculated according to Lambert–Beer's law.

#### Dynamic Light Scattering

DLS experiments were carried out using an ALV 5000E instrument. All measurements were performed at room temperature using a krypton laser (Spectra Physics) of wavelength 647.1 nm. Its output varied between 100 and 300 mW depending on scattering strength. Correlation functions were measured in steps of 30° in the range 60–150°. Every angle was measured for 120 s to obtain a smooth correlation function. Correlations were analyzed using CONTIN.<sup>[21]</sup>

#### Atomic Force Microscopy

AFM imaging in non-contact mode was done on a Solver P47H (NTMDT) using NSG11-B tips from NTMDT. Samples were prepared by drop-casting from methanol solutions (1.3–1.8 × 10<sup>-5</sup> mol L<sup>-1</sup>) onto an Si-wafer.

#### Circular Dichroism

CD spectra were recorded on a Jasco J-715 spectropolarimeter equipped with a Jasco PTC-348WI temperature-controlled cell. Details of the CD experiments have been published before.<sup>[11]</sup>

#### Analytical Ultracentrifugation

Sedimentation equilibrium experiments were performed in a Beckman Optima XL-A analytical ultracentrifuge using Epon six- or two-channel centrepieces with a path length of 1.2 cm in combination with an An-60Ti rotor. The sample volume was 130 or 200 μL. The rotor speed was 9000, 30 000, or 32 000 rpm, and the rotor temperature was 20°C. Absorbance versus radius data, *A(r)*, were measured at 278 nm in experiments on the apo-peptide and at 485 or 555 nm in the case of the metalloprotein. Experiments on the metalloprotein were carried out in 100% PBS buffer at initial concentrations of 31, 78, and 118 μM, and in PBS containing 50% (v/v) ethanol at an initial concentration of 33 μM. Experiments on the apo-peptide were performed in 100% PBS including 1 mM hydroxyethylethylenediaminetriacetic acid (HEDTA) and in ethanol/PBS (1 : 1 v/v) including 1 mM HEDTA at an initial concentration of 36 μM. The partial specific volumes of the apo-peptide and metalloprotein in aqueous buffers and in solvents containing 50% ethanol were calculated<sup>[22]</sup> to be 0.776 and 0.805 mL g<sup>-1</sup>, respectively. The *A(r)* data were evaluated as described earlier,<sup>[19,22,23]</sup> using the computer program DISCREEQ by Schuck.<sup>[24]</sup> Buffer densities were calculated using the software Sednterp.<sup>[25]</sup>

#### Synthesis of Apo-peptide

Peptide synthesis was performed on an Applied Biosystems 433A peptide synthesizer, using standard Fmoc chemistry on a Rink Amide AM resin. The amino acid residues were used as free acids, and coupling was facilitated by HBTU and HOBT. A *tert*-butyl group was chosen as a side-chain protective group for the glutamic acid and tyrosine residues. The ε-amino group of lysine residues was protected with a *tert*-butoxycarbonyl group. 6-(2,2':6',2''-Terpyridin-4'-yloxy)hexanoic acid was used as the *N*-terminal capping reagent. After completion of the desired amino acid sequence, treatment of the resin-bound product with 50% trifluoroacetic acid in dichloromethane simultaneously cleaved the linker and removed the protective groups of the side chain. In this way, a peptide with a C-terminal amide group was obtained. After filtration of the resin, the solvents were evaporated to near dryness. Subsequent precipitation with cold diethyl ether resulted in a white powder. The peptide was purified by dialysis in, first, distilled water containing approximately 6 M Gdn · HCl for denaturation and NaOH (added until a clear solution was obtained) for solubility, and second, pure distilled water to remove the additional salts. Water was removed by lyophilization. Typically, after a synthesis on a 0.25 mmol scale, 270 mg (55%) of pure apo-peptide was obtained as a white powder. *m/z* (MALDI-TOF) 2867 g mol<sup>-1</sup> [M(Na<sup>+</sup>)]. UV-vis (PBS, pH 7.4) λ<sub>max</sub> 291 nm, ε<sub>280</sub> 1.21 × 10<sup>4</sup> M<sup>-1</sup> cm<sup>-1</sup>.

#### Synthesis of Bis(apo-peptide)iron(II) Hexafluorophosphate

To a solution of the apo-peptide (100 mg, 35.1 μmol) in methanol (25 mL) was added FeSO<sub>4</sub> · 7H<sub>2</sub>O (4.9 mg, 17.6 μmol) suspended in methanol (1 mL). The colourless reaction mixture immediately turned purple. After being stirred at room temperature under argon for 12 h, excess NH<sub>4</sub>PF<sub>6</sub> (146 mg, 0.894 mmol) was added as a solution in methanol. After additional stirring for 4 h, the solvent was evaporated until near-dryness. Precipitation with ice-cold diethyl ether yielded 200 mg (94%) of bis(apo-peptide)iron(II) hexafluorophosphate as a purple solid. *m/z* (MALDI-TOF) 5750 g mol<sup>-1</sup> [M<sup>+</sup> - PF<sub>6</sub><sup>-</sup>]. λ<sub>max</sub> (PBS, pH 7.4) 561, 329, 291 nm, ε<sub>561</sub> 3.79 × 10<sup>3</sup> M<sup>-1</sup> cm<sup>-1</sup>.

#### Acknowledgments

This work was supported by the Fonds der Chemischen Industrie (Kékulé Fellowship for G.V., Forschungsbeihilfe U.S.S.), the International Max Planck Research School, the Deutsche Forschungsgemeinschaft [Emmy Noether-Program (H.-A.K.), SFB 486 (U.S.S.)], and the Dutch Polymer Institute (U.S.S.). BASF AG (Ludwigshafen, Germany) is acknowledged for donating NMP. The authors are grateful to Dr S. Wiegand and B. Müller for carrying out DLS measurements.

#### Accessory Materials

Further experimental results are available from the author or, until January 2009, from the *Australian Journal of Chemistry*.

#### References

- [1] (a) W. F. DeGrado, C. M. Summa, M. Pavone, F. Nistri, A. Lombardi, *Annu. Rev. Biochem.* **1999**, *68*, 779. doi:10.1146/ANNUREV.BIOCHEM.68.1.779  
(b) G. Xing, V. J. DeRose, *Curr. Opin. Chem. Biol.* **2001**, *5*, 196. doi:10.1016/S1367-5931(00)00190-3  
(c) Y. Lu, S. M. Berry, T. D. Pfister, *Chem. Rev.* **2001**, *101*, 3047. doi:10.1021/CR0000574
- [2] G. Parraga, S. J. Horvath, A. Eisen, W. E. Taylor, L. Hood, E. T. Young, R. E. Klevit, *Science* **1988**, *241*, 1489.
- [3] A. Fedorova, A. Chaudhari, M. Y. Ogawa, *J. Am. Chem. Soc.* **2003**, *125*, 357. doi:10.1021/JA026140L

- [4] (a) M. Gochin, V. Khorosheva, M. A. Case, *J. Am. Chem. Soc.* **2002**, *124*, 11 018. doi:10.1021/JA020431C  
(b) W. D. Kohn, C. M. Kay, B. D. Sykes, R. S. Hodges, *J. Am. Chem. Soc.* **1998**, *120*, 1124. doi:10.1021/JA973673Z
- [5] G. R. Dieckmann, D. K. McRorie, D. L. Tierney, L. M. Utschig, C. P. Singer, T. V. O'Halloran, J. E. Penner-Hahn, W. F. DeGrado, V. L. Pecoraro, *J. Am. Chem. Soc.* **1997**, *119*, 6195. doi:10.1021/JA964351I
- [6] M. W. Mutz, G. L. McLendon, J. F. Wishart, E. R. Gaillard, A. F. Corin, *Proc. Natl. Acad. Sci. U. S. A.* **1996**, *93*, 9521. doi:10.1073/PNAS.93.18.9521
- [7] (a) M. Lieberman, M. Tabet, T. Sasaki, *J. Am. Chem. Soc.* **1994**, *116*, 5035.  
(b) M. R. Ghadiri, C. Soares, C. Choi, *J. Am. Chem. Soc.* **1992**, *114*, 825.  
(c) M. Lieberman, T. Sasaki, *J. Am. Chem. Soc.* **1991**, *113*, 1470.  
(d) M. R. Ghadiri, M. A. Case, *Angew. Chem. Int. Ed. Engl.* **1993**, *32*, 1594.  
(e) R. Schnepf, P. Hörth, E. Bill, K. Wieghardt, P. Hildebrandt, W. Haehnel, *J. Am. Chem. Soc.* **2001**, *123*, 2186. doi:10.1021/JA001880K
- [8] T. Koide, M. Yuguchi, M. Kawakita, H. Konno, *J. Am. Chem. Soc.* **2002**, *124*, 9388. doi:10.1021/JA026182+
- [9] A. Lupas, *Trends Biochem. Sci.* **1996**, *21*, 375. doi:10.1016/0968-0004(96)10052-9
- [10] (a) U. S. Schubert, C. Eschbaumer, *Angew. Chem.* **2002**, *114*, 3016; *Angew. Chem. Int. Ed.* **2002**, *41*, 2892. doi:10.1002/1521-3773(20020816)41:16<2892::AID-ANIE2892>3.0.CO;2-6  
(b) B. G. G. Lohmeijer, U. S. Schubert, *Angew. Chem.* **2002**, *114*, 3980; *Angew. Chem. Int. Ed.* **2002**, *41*, 3825. doi:10.1002/1521-3773(20021018)41:20<3825::AID-ANIE3825>3.0.CO;2-6
- [11] G. W. M. Vandermeulen, C. Tziatzios, H.-A. Klok, *Macromolecules* **2003**, *36*, 4107. doi:10.1021/MA034124I
- [12] (a) E. C. Constable, M. D. Ward, *J. Chem. Soc., Dalton Trans.* **1990**, 1405.  
(b) G. R. Newkome, F. Cardullo, E. C. Constable, C. N. Moorfield, A. M. W. C. Thompson, *J. Chem. Soc., Chem. Commun.* **1993**, 925.  
(c) G. R. Newkome, E. F. He, *J. Mater. Chem.* **1997**, *7*, 1237. doi:10.1039/A700127D  
(d) P. R. Andres, R. Lunkwitz, G. R. Pabst, K. Böhn, D. Wouters, S. Schmatloch, U. S. Schubert, *Eur. J. Org. Chem.* **2003**, 3769. doi:10.1002/EJOC.200300327
- [13] (a) U. S. Schubert, M. Heller, *Chem. Eur. J.* **2001**, *7*, 5252. doi:10.1002/1521-3765(20011217)7:24<5252::AID-CHEM52-52>3.0.CO;2-9  
(b) U. S. Schubert, C. Eschbaumer, P. R. Andres, H. Hofmeier, C. H. Weidl, E. Herdtweck, E. Dulkeith, A. Morteani, N. E. Hecker, J. Feldman, *Synth. Metab.* **2001**, *121*, 1249. doi:10.1016/S0379-6779(00)01430-2
- [14] (a) K. Naka, A. Kobayashi, Y. Chujo, *Macromol. Rapid Commun.* **1997**, *18*, 1025. doi:10.1002/MARC.1997.030181205  
(b) J. J. S. Lamba, C. L. Fraser, *J. Am. Chem. Soc.* **1997**, *119*, 1801. doi:10.1021/JA962834G
- [15] (a) Y.-H. Chen, J. T. Yang, H. M. Martinez, *Biochemistry* **1972**, *11*, 4120.  
(b) Y.-H. Chen, J. T. Yang, K. H. Chau, *Biochemistry* **1974**, *13*, 3350.
- [16] J. Y. Su, R. S. Hodges, C. M. Kay, *Biochemistry* **1994**, *33*, 15 501.
- [17] D. R. Benson, B. R. Hart, X. Zhu, M. B. Doughty, *J. Am. Chem. Soc.* **1995**, *117*, 8502.
- [18] (a) L. N. M. Duysens, *Biochim. Biophys. Acta* **1956**, *19*, 1. doi:10.1016/0006-3002(56)90380-8  
(b) A. S. Schneider, D. Harmatz, *Biochemistry* **1976**, *15*, 4158.
- [19] (a) D. Schubert, P. Schuck, *Prog. Colloid Polym. Sci.* **1991**, *86*, 12.  
(b) P. Schuck, B. Legrum, H. Passow, D. Schubert, *Eur. J. Biochem.* **1995**, *230*, 806.
- [20] T. L. Williams, C. Fenselau, *Eur. Mass Spectrom.* **1998**, *4*, 379.
- [21] S. Provencher, *Comput. Phys. Commun.* **1982**, *27*, 213. doi:10.1016/0010-4655(82)90173-4
- [22] H. Durchschlag, in *Thermodynamic Data for Biochemistry and Biotechnology* (Ed. H.-J. Hinz) **1986**, pp. 45–128 (Springer: Berlin).
- [23] (a) G. Musco, C. Tziatzios, P. Schuck, A. Pastore, *Biochemistry* **1995**, *34*, 553.  
(b) I. Collinson, C. Breyton, F. Duong, C. Tziatzios, D. Schubert, E. Or, T. Rapoport, W. Kühlbrandt, *EMBO J.* **2001**, *20*, 2462. doi:10.1093/EMBOJ/20.10.2462
- [24] P. Schuck, *Prog. Colloid Polym. Sci.* **1994**, *94*, 1.
- [25] T. M. Laue, B. D. Shah, T. M. Ridgeway, S. L. Pelletier, in *Analytical Ultracentrifugation in Biochemistry and Polymer Science: Computer-Aided Interpretation of Analytical Sedimentation Data for Proteins* (Eds S. E. Harding, A. J. Rowe, J. C. Horton) **1992**, pp. 90–125 (Royal Society of Chemistry: Cambridge).